Core-hole effects on energy-loss near-edge structure

G. Duscher[a,b], R. Buczko[a,b], S.J. Pennycook[a,b], S.T. Pantelides[a,b]

[a] *Department of Physics and Astronomy, Vanderbilt University, Nashville, TN, USA*
[b] *Solid State Division, Oak Ridge National Laboratory, Oak Ridge, TN, USA*

Abstract

We present first-principles electron energy-loss near-edge structure calculations that incorporate electron–hole interactions and are in excellent agreement with experimental data obtained with X-ray absorption spectroscopy (XAS) and electron energy-loss spectroscopy (EELS). The superior energy resolution in XAS spectra and the new calculations make a compelling case that core-hole effects dominate core-excitation edges of the materials investigated: Si, SiO_2, MgO, and SiC. These materials differ widely in the dielectric constant leading to the conclusion that core–hole effects dominate all core-electron excitation spectra in semiconductors and insulators. The implications of the importance of core-holes for simulations of core-electron excitation spectra at interfaces will be discussed. © 2001 Elsevier Science B.V. All rights reserved.

1. Introduction

Electron energy loss spectroscopy (EELS) is now a standard tool to investigate the local chemistry and bonding of defects in solids. The energy thresholds of the ionization edges in EELS spectra are determined by the identity of the element [1]. The area under the edges can be used to extract the chemical composition, while threshold shifts are induced by different bonding coordination and charge states [2]. The shapes of ionization edges in EELS spectra, the electron energy-loss near-edge structure (ELNES), reflect the available excited states which depend on the local bonding environments.

Because of the complex relationship of the electronic structure to symmetry an easy inter-pretation of the ELNES changes in terms of bonding is only possible in limited cases. Early work suggested that one should calculate the (angular-momentum-resolved) density of states (DOS) of the conduction band, which can be obtained with band structure calculations to simulate the ELNES or the X-ray absorption near edge structure (XANES) [3]. The agreement between experiment and theory proved to be misleading when the threshold for transitions to band states was extracted from photoemission data [4]. It was concluded that excitonic effects dominate these spectra [4]. Even though the $Z + 1$ approximation was used in a number of studies (for example [5–9]), no definite conclusions have been drawn concerning when core–hole effects must be included in calculations. Here, we

investigate the role of core holes for semiconductors and insulators with a range of dielectric constants.

The high spatial resolution and the high sensitivity for light elements make EELS ideal to investigate segregation to extended defects like internal interfaces. The combination of Z-contrast imaging and theoretical calculations proved to be successful for extracting the local atomic structure of interfaces [10]. The Z-contrast imaging serves as input for the atomic configuration at internal interfaces; theory refines the atomic positions. Light elements like oxygen, carbon and nitrogen are, however, mostly not visible in Z-contrast images and thus many possible structures must be probed. To check the results of such calculations it seems helpful to calculate the band structure, to simulate the ELNES side by side, and to compare it with the experimental data.

So far, there are a few examples of interfaces studied with this approach. A cluster method has been used to calculate the ELNES at metal–alumina interfaces and compared to EELS spectra obtained with the spatial difference technique [11,12]. But even in bulk calculations, ELNES simulated in terms of the conduction band DOS have not shown acceptable agreement to experiments in most non-metallic materials. In this paper we will show that excellent agreement can be achieved by inclusion of a local approximation of the core hole effect into an ab initio fully self-consistent LDA calculation. A comparison of all electron-calculations with pseudopotential calculations is used to check the theory, and to determine physical parameters. The agreement between theory and experiment for the EELS and XAS K and $L_{2,3}$ edges in several materials is excellent and electronic structure conclusions can be drawn. The method is simple enough to be used at interfaces.

2. Method

The EELS spectra were recorded on a VG HB501 UX with 100 kV acceleration voltage and a cold field emission source. Two spectrometers were used: a Gatan PEELS 666 and a VG serial EELS

modified for parallel detection according to the design of McMullan [13]. The detector was either a photodiode array or a CCD camera. The valence-loss spectra were recorded for each spectrum to ensure low surface contributions and, if necessary, were used to obtain the single scattering contribution. Several spectra (usually 10) were added after inspection for electron beam damage to improve signal to noise ratio.

We used two self-consistent methods both founded on density functional theory and the local density approximation. We used a full-potential linearized augmented plane wave code [14] (FLAPW) and a pseudopotential code with plane wave basis set [15] to calculate the band structure and angular momentum projected density of states for different atoms in the periodic supercell.

To calculate the angular-momentum-projected density of states of an atom in the ground state one can use the primitive crystal cell. To study the effects of a core-hole, we have to choose one atom in which the hole is localized. A supercell has to be used that is large enough to minimize any unphysical interaction between these excited atoms. For this reason we used supercells of increasing sizes until convergence of the results was achieved. We introduced a core hole explicitly in a particular atom; an electron is placed in the conduction band with a hole in a core level. An all-electron calculation such as the FLAPW method used here is most suitable for this task.

We also performed calculations in which the core hole was approximated by an extra proton on the nucleus ($Z + 1$ approximation) [6]. These calculations were performed with both the FLAPW method and the plane-wave pseudopotential method. In all calculations, the number of k points in the Brillouin zone was always large enough to produce a smooth DOS after convolution with a 0.2 eV wide Gaussian. To compare the calculations with EELS experiments a broadening of 0.5 eV was applied.

It should be noted that these calculations are possible only for core excitations; they would not be appropiate for transitions from the valence bands where delocalization of the hole makes it necessary to use a more sophisticated excitation

Table 1
The relevant parameters of the calculations for the different materials. The parameters for Wien97 are the muffin tin sphere radius R_{mt} and the $Rk_{max}(= R_{mt} * k_{max})$ value, while for VASP the cut off energy and the projection radius are shown

Material	Element	R_{mt} spheres (a.u.)	Rk_{max}	Cutoff (eV)	Projection radius (Å)
Silicon	Si	2.0	8	150	1.5
Quartz	Si	1.6	6	300	1.4
Quartz	O	1.35	6	300	0.8
MgO	Mg	2.1	8	350	1.1
MgO	O	1.8	8	350	1.1

Fig. 1. Experimental and theoretical X-ray absorption spectra of the Si-$L_{2,3}$ edge. Thick gray curve: experiment [16]; thick black curve (core–hole): full calculation including electron–hole interactions with a self-consistent hole orbital; thin black curve ($Z + 1$): calculation using the $Z + 1$ model; dotted curve (Z): calculation of excitation spectrum without electron-hole interactions; dash–dot curve (EM band): effective-mass (parabolic band) spectrum without electron–hole interactions; long-dash curve (EM exciton): effective-mass spectrum with hydrogenic excitonic effects as first done by Altarelli and Dexter [5].

theory as for example the Bethe–Salpeter equation [8]. These methods are computationally much more expensive.

We chose Si, SiO_2 and MgO because they have been studied extensively both experimentally and theoretically, but controversies still exist about the nature of the ELNES (as we will discuss for each material separately). The dielectric constant decreases from Si to SiO_2, which should result in different screening of the core–hole. Because the electronic structure of the ground state of all these materials is theoretically well documented we do not go into the details of this, but just state that we can reproduce the most recent calculations with both theoretical methods. The parameter for the calculations are shown in Table 1. The experimental EELS and XAS edges are also compared with the literature and no discrepancy could be found except for the different energy resolution obtained in the spectra shown here. The next section will present and discuss the results for the materials under investigation one by one.

3. Results and discussion

We first consider the Si-$L_{2,3}$ edge in silicon. Even though the band structure of silicon is well known, the nature of the Si-L_3 ELNES has been controversial. Initially, the Si-$L_{2,3}$ XANES was compared with the total DOS of silicon, but the agreement was poor [16]. Later, effective mass excitons [5] or the projected DOS [17] were used to
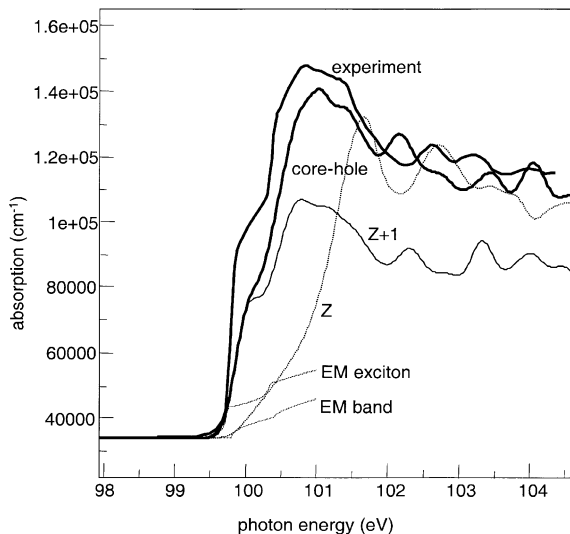
explain the Si-$L_{2,3}$ ELNES. We compared the results of these suggestions with those including localized excitonic effects. In Fig. 1, we present Si-$L_{2,3}$ ELNES simulations with different degrees of sophistication. In the following we explain these simulations in decreasing order of sophistication and compare them with the experimental XANES (thick black line in Fig. 1):

(a) The most accurate method used is the calculation with an explicit core hole. In the all-electron method, it is possible to place an electron from one core state into the conduction band. The supercell had to be increased to 64 atoms before the electronic structure converged with size. With this approach, the theory is in excellent agreement with not only the shape, but also the absolute absorption coefficient with photon energy.

The formula to calculate the absorption coefficient is

$$4\pi^2 \alpha h \omega a_B^2 N/V 1/3 \Sigma_{l'=l\pm1} 1/(2l'+1)[(1+1)$$
$$\delta_{l',l+1} + l\delta_{l',l-1}]D_{l'}(R_{nl}^{n'l'})^2,$$

where N is the number of atoms of the same type, V the unit cell volume, $D_{l'}$ the projected DOS, $R_{nl}^{n'l'}$ the radial integral.

The sum in this formula is calculated with Wien97 (please note that there was an error in Wien97, which is corrected with version Wien97.10, September 2000).

The onset of the simulated ELNES was placed at 99.8 eV as found by XAS data and which agrees with the energy calculated from the PES and band gap following Ref. [4]. This theoretical spectrum agrees in position, intensity and shape with the experimental ELNES. Such a level of agreement between experiment and theory of core-excitation edges is unusual.

(b) We also performed calculations with the $Z+1$ approximation. The results of the FLAPW and pseudopotential method are in agreement and thus only the theoretical edge obtained with the FLAPW method is shown in Fig. 1 (Fig. 2 shows the one obtained with the pseudopotential method). The position and shape of the core-excitation edge (marked with $Z+1$ in Fig. 1) agrees well with the experiment and the explicit core-hole simulation. The main discrepancy in this result is too low an intensity, although this level of agreement is sufficient for comparison with experimental ELNES edges where the absolute intensity is hard to obtain.

(c) The next lower level of sophistication for core excitations is to eliminate the electron hole interactions and calculate the full spectrum between the core level and the perfect crystal conduction band Bloch states. This theoretical ELNES is labeled Z in Fig. 1. This result is very similar to the weighted sum of s and d PDOS (without consideration of any excitonic effects) as reported by Weng et al. [17]. When positioned at the correct energy, the agreement between this simulation and experiment is poor. Weng et al. [17] reported a reasonable
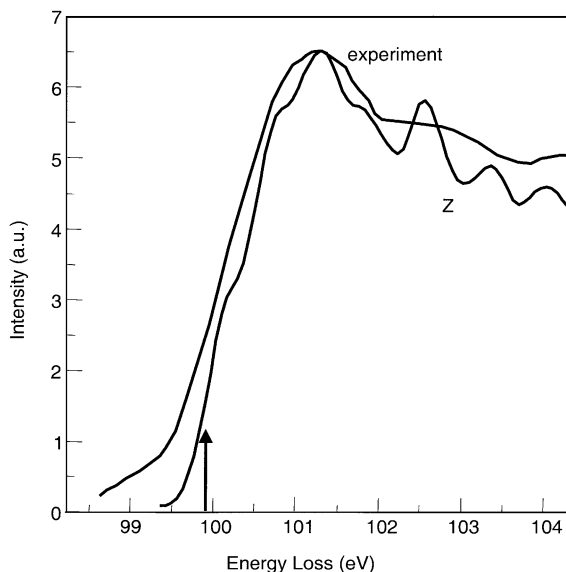

Fig. 2. Experimental and theoretical Si-L$_{2,3}$ edges. Gray curve: experimental curve obtained with a VG Microscope HB501 UX using 100 kV acceleration voltage and collection semiangle of 13 mrad; black curve: theoretical spectrum using the PDOS as described in the text.

agreement between the PDOS and ELNES because of two factors: the limited resolution in EELS and the arbitrary positioning of the onset of the simulated edge. Fig. 2 reproduces the result of Weng et al. [17] and one can see that this arbitrary shift leads to states below the conduction band minimum as calculated from PES and the band gap (indicated by the arrow in Fig. 2). The PDOS does not differ much from the total DOS, which was found to be not in agreement with the XANES by Brown and Rustgi [16].

(d) The above results let us to conclude that the core-hole effect dominates the Si-L$_{2,3}$ XANES and ELNES. To explore the possibility of a delocalized (effective mass) core hole, we reproduced the work of Altarelli and Dexter [5], using the matrix element calculated by FLAPW. The result of this calculation is seen in Fig. 1 (marked effective mass). This approach can reproduce the steep rise of the Si-L$_{2,3}$ edge at the onset, but the absorption coefficient is nearly an order of magnitude too

low (as noted by Alterelli and Dexter [5]). We therefore exclude the possibility of a major influence of the Si-L_3 edge by delocalized excitonic effects.

The agreement (Fig. 1) between the experimental XANES and the explicit core hole method (a) shows that the Si-$L_{2,3}$ edge onset is dominated by *localized* excitonic effects which can be approximated well with the $Z + 1$ approximation (method (b) above) [18]. To explore the universality of this finding we will in the following compare the methods (b), and (c) for $L_{2,3}$ and K edges of materials with smaller dielectric constants. In these materials, where the screening of the core hole is lower than in silicon, we expect an even higher influence of excitonic effects on the core excitation edges.

The approach taken in the following is to calculate the transition matrix elements with the FLAPW code to get the weighting factors for s and d PDOS. The edge onset is calculated as the difference between the energy of a supercell with and without an atom including an explicit core hole. The onset calculated this way has been found to be in agreement with the onset of XAS and EELS edges within 1% [19]. These FLAPW calculations can be performed with rather small supercells (16 atoms). The angular momentum density of states is then calculated with the more efficient pseudopotential method in the $Z + 1$ approximation to save computer time. The size of the supercell was increased until convergence was reached. This approach has the advantage that it is efficient enough to handle the large supercells required for calculations of interfaces.

The results of these calculations were always compared with Z calculations (no core-hole effects) to test whether local excitonic effects have to be included. The Z calculated edge simulations were positioned at the experimentally value determined by XPS measurements and the band gap following Ref. [4]. Any discrepancy in position or shape is the result of core-hole effects. The relevant parameters for the calculations are composed in Table 1.

First we explore the Si-$L_{2,3}$ edge of SiO_2 (quartz). This edge has recently been reported to
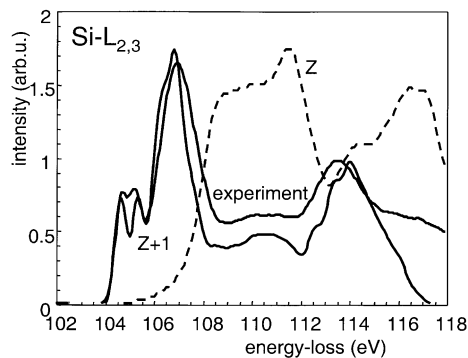

Fig. 3. The Z and $Z + 1$ theoretical Si-$L_{2,3}$ spectra compared with the experimental spectrum of quartz [20]. The smearing is 0.3 eV in the theoretical spectrum.

be reproduced well with PDOS calculations without the inclusion of a core hole effect [20]. We find that inclusion of the electron–hole interaction in the $Z + 1$ approximation improves dramatically the agreement between theory and experiment. The results of the Z (method (c); the same approximation as used by Garvie et al. [20]) and $Z + 1$ calculations are compared in Fig. 3; we notice again that as in the case of silicon, local excitonic effects dominate the near-edge structure.

We applied the same scheme to the O-K edge of SiO_2. K edges are easier to calculate as only transitions from the 1 s to states with p symmetry are allowed within the dipole selection rule. The O-K edge is widely considered not to be influenced by the core hole effect [20–23,7]. The comparison of the experimental O-K ELNES of SiO_2 with the simulation in Fig. 4 shows clearly that core hole effects have to be included to describe this edge. A supercell containing 72 atoms was needed to reach convergence in size. The comparison of the calculated and experimental Si-K edge in silicon and quartz shown in Figs. 5 and 6 proves again the dominance of the core hole effect. In these figures we intentionally used a small amount of broadening to show more structure that may be resolved by XAS. Clearly more broadening would improve agreement with experiment.

To confirm the approach taken in this paper we calculated the edges of MgO, an ionic material with a dielectric constant between Si and SiO_2.
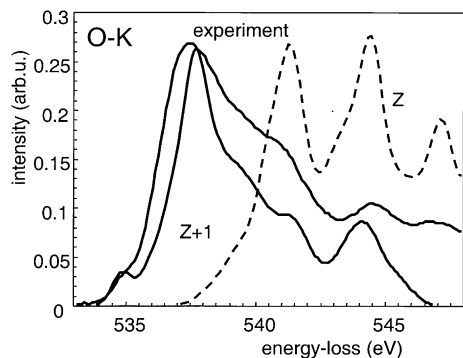
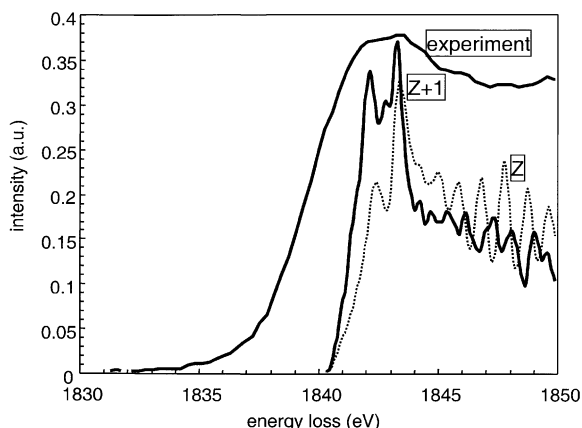Fig. 4. The Z and $Z+1$ theoretical O-K spectra compared with the experimental spectrum of quartz [20].

Fig. 6. The Z and $Z+1$ theoretical Si-K spectra compared with the experimental spectrum of silicon.
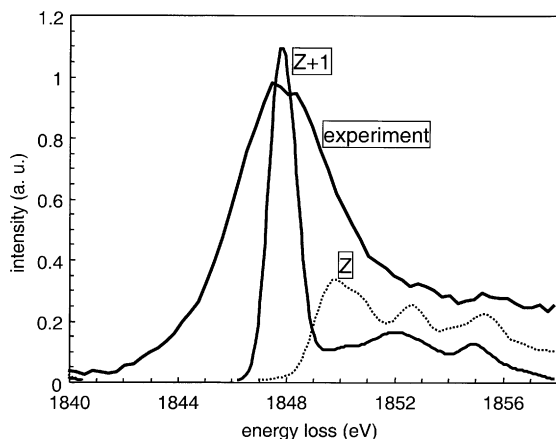

Fig. 5. The Z and $Z+1$ theoretical Si-K spectra compared with the experimental spectrum of amorphous SiO_2.

Fig. 7. The Z and $Z+1$ theoretical O-K spectra compared with the experimental spectrum of MgO.

Again this system is well known and bears no surprises in the electronic structure. The ELNES of the Mg-K, and O-K edges have been calculated with both cluster approaches [7,24] and a periodic supercell approach [9], but agreement with experiment was rather poor. We used the $Z+1$ calculation and the effective core hole in the FLAPW method to simulate the ELNES. We did not calculate the Mg-$L_{2,3}$ edges of MgO, because the Mg $2p$ and Mg $2s$ states must be treated as a semi-core state in the FLAPW. This indicates that a core hole in these states is no longer localized enough to be described by the $Z+1$ or the explicit
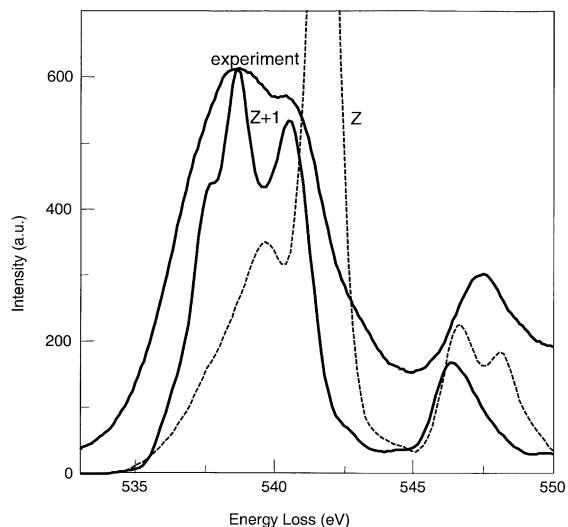
core hole methods. The agreement between theory and ELNES of the Mg-K and O-K edge (Figs. 7 and 8) again is remarkable. The cluster method could not find any difference between a $Z+1$ approximation and the unexcited atom [7]. This is probably due to the lack of self-consistency of this method or insufficient representation of the bulk with a cluster. More recently, Mizoguchi et al. [24] reported Z, $Z+1$ and $Z+1/2$ spectra and could
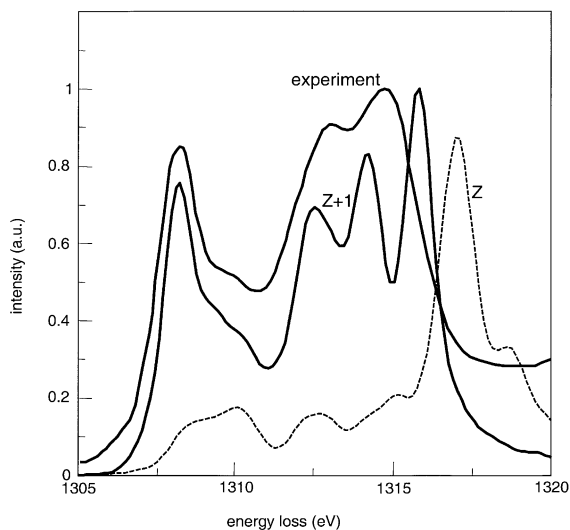
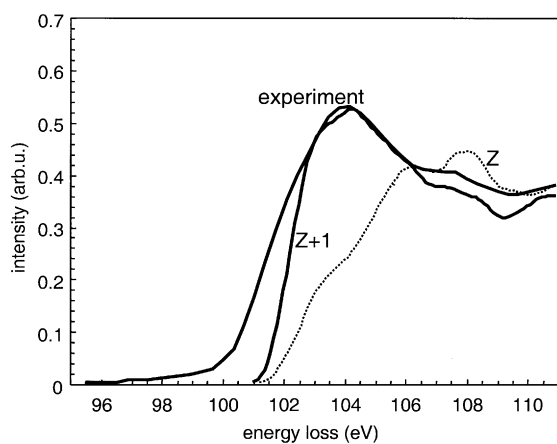Fig. 8. The Z and $Z+1$ theoretical Mg-K spectra compared with the experimental spectrum of MgO.

Fig. 9. The Z and $Z+1$ theoretical Si-$L_{2,3}$ spectra compared with the experimental spectrum of SiC.

approximation can not reproduce the shape, while the $Z+1$ approximation agrees very well with experiment.

The $Z+1$ approximation seems to be necessary in all non-metallic materials for all edges of deep core excitations. The next step will be to use the theoretical methods described in this paper to determine the ELNES at interfaces, e.g. the Si–SiO_2 or SiC–SiO_2 interface and compare the results for different local bonding arrangements. Comparison with experimental ELNES should allow a determination of which bonding arrangements are present at real interfaces.

4. Conclusion

We have reached a level of agreement between theory and experiment not achieved previously in such a range of different materials. This was achieved by including a localized core-hole effect. There was no significant difference between both the methods used, a core hole in an all-electron method and the $Z+1$ approximation. This combination of methods allows the matrix elements to be determined from all-electron calculations with limited resolution, and accurate spectra to be calculated with the faster pseudopotential approach. This approach is sufficiently robust to proceed to interface structures. It is anticipated that structure determination of interfaces will make a significant leap forward using this approach involving the combination of Z-contrast imaging, EELS and state of the art density functional calculations.

not reproduce the data very well, again probably because they used a small cluster that is not representative of a true solid.

The poor results of the mixed basis set calculations are probably due to the rather small supercells (8 atoms) [9]. In our calculations we reached convergence only with a supercell of 64 atoms.

As a last example we discuss the Si-$L_{2,3}$ edge of silicon carbide. The experimental and theoretical ELNES is shown in Fig. 9. Obviously the Z

References

[1] R.F. Egerton, Electron Energy-Loss Spectroscopy in the Electron Microscope, Plenum Press, New York, 1996.

[2] H.J. Himpsel, F.R. McFeel, A. Taleb-Ibrahimi, J.A. Yarmoff, G. Hollinger, Phys. Rev. B 38 (1988) 6084.

[3] F.C. Brown, C. Cahwiller, A.B. Kunz, N.O. Lipari, Phys. Rev. Lett. 25 (14) (1970) 927.

[4] S.T. Pantelides, Phys. Rev. B 11 (1975) 2391.

[5] M. Altarelli, D.L. Dexter, Phys. Rev. Lett. 29 (1972) 1100.

[6] H.P. Hjalmarson, H. Buttner, J.D. Dow, Phys. Rev. B 4 (1981) 6010.

[7] T. Lindner, H. Sauer, W. Engel, K. Kambe, Phys. Rev. B 33 (1986) 22.

[8] E.L. Shirley, Phys. Rev. Lett. 80 (1998) 794–796.

[9] S. Köstlmeier, C. Elsässer, B. Meyer, Ultramicroscopy 80 (1999) 145.

[10] Y. Yan, M.F. Chisholm, G. Duscher, A. Maiti, S.J. Pennycook, S.T. Pantelides, Phys. Rev. Lett. 81 (1998) 3675.

[11] R. Brydson, J. Bruley, H. Müllejans, C. Scheu, M. Rühle, Ultramicroscopy 59 (1996) 81.

[12] C. Scheu, G. Dehm, M. Rühle, R. Brydson, Philos. Mag. A 78 (1998) 438.

[13] D. McMullan, J.M. Rodenburg, Y. Murooka, A.J. McGibbon, EMAG-MICRO 89, Proceedings of the Institute of Physics Electron Microscopy and Analysis Group and Royal Microscopical Society Conference, London, UK, 13–15 September 1989, 1990, pp. 55–58.

[14] P. Blaha, K. Schwarz, J. Luitz, WIEN97, A Full-Potential Linearized Augmented Plane Wave Package for Calculating Crystal Properties, Karlheinz Schwarz, Techn. Univ. Wien, Austria, 1999. ISBN 3-9501031-0-4.

[15] VASP, Phys. Rev. B 55 (1996) 11169.

[16] F.C. Brown, O.P. Rustgi, Phys. Rev. Lett 28 (1972) 497.

[17] X. Weng, P. Rez, O.F. Sankey, Phys. Rev. B 40 (1989) 5694.

[18] R. Buczko, S.J. Pennycook, G. Duscher, S.T. Pantelides, Phys. Rev. Lett. 85 (2000) 2168.

[19] R. Buczko, S.J. Pennycook, G. Duscher, S.T. Pantelides, Appl. Phys. Lett. (2000), submitted for publication.

[20] L.A.J. Gravie, P. Rez, J.R. Alvarez, P. Buseck, A.L. Craven, American Mineralogist 85 (2000) 732.

[21] D.A. Muller, T. Sorsch, S. Moccio, F.H. Baumann, K. Evans-Lutterodt, G. Timp, Nature 399 (1999) 758.

[22] J.B. Neaton, D.A. Muller et al, Phys. Rev. Lett. 85 (2000) 1298.

[23] D.J. Wallis, P.H. Gaskell, and R. Brydson, in: A.J. Craven (Ed.), Electron Microscopy and Analysis 1993 Proceedings of the Institute of Physics Electron Microscopy and Analysis Group Conference, Liverpool, UK, 14–17 September 1993, pp. 47–50.

[24] T. Mizoguchi, I. Tanaka, M. Yoshiya, F. Oba, K. Ogasawara, H. Adachi, Phys. Rev. B 61 (2000) 2180.